Korean J. of Chem. Eng., **13**(6), 612-619 (1996)

MATHEMATICAL MODELING OF FED-BATCH BUTANOL FERMENTATION WITH SIMULTANEOUS PERVAPORATION

Chang-Ho Park* and Charles Q. Geng†

*Department of Chemical Engineering, The Institute of Material Science and Technology, Kyung Hee University, Yongin-Si 449-701, Korea
The Pillsbury Technology Center, 330 Univ. Ave. S.E., Minneapolis, MN 55414, U.S.A.
(Received 4 June 1996 • accepted 26 August 1996)

Abstract – A mathematical model was developed to describe a fed-batch acetone-butanol-ethanol (ABE) fermentation with simultaneous pervaporation. The model predicted satisfactorily batch or fed-batch fermentation with or without pervaporation by introducing a parameter reflecting cell activity loss during fed-batch fermentation with pervaporation. The model also predicted the effect of membrane area, membrane thickness, and sweep air flow rate on glucose consumption rate and residual butanol concentration in the fermentation broth. Glucose consumption rate increased by 30% by either doubling the membrane area or decreasing membrane thickness by half.

Key words : Mathematical Model, Butanol Fermentation, Prevaporation, Membrane Area and Thickness, Sweep Air Flow Rate

INTRODUCTION

Butanol fermentation is rather complicated in its pathway and served as a good example for mathematical modeling in fermentation. Volesky and co-workers [Votruba et al., 1986] pioneered modeling of batch butanol fermentation processes using Monod's growth model. The model was modified to include product inhibition and pH effect on acid re-utilization [Srivastava and Volesky, 1990], and further modified for simulation of fed-batch butanol fermentation [Volesky and Votruba, 1992]. Continuous ABE fermentation with incorporation of butyrate and butanol inhibition was modeled by Jarzebski et al. [1992].

Simultaneous fermentation and separation systems were also modeled mathematically. Simultaneous fermentation and separation increases productivity by removing components from the culture medium. Shukla et al. [1989] modeled ABE fermentation in a continuous hollow fiber fermenter-extractor. Groot et al. [1991] modeled continuous isopropanol-butanol-ethanol (IBE) fermentation with pervaporation by lumping all solvent products in one parameter. Park et al. [1991] used an equilibrium stage approach to model a trickle bed fermentor-separator using gas stripping.

In this study, we developed a mathematical model that describes a fed-batch butanol fermentation with simultaneous pervaporation and studied separation conditions that increase glucose consumption. Pervaporation is one of simultaneous fermentation and separation technique and can be used to increase fermentation productivity. Pervaporation is a membrane separation process that combines evaporation and permeation through a semipermeable membrane, and azeotropic point can be avoided because the vapor-liquid equilibrium is modified when a polymeric membrane is placed between the two phases of a binary mixture. We compared the prediction by the mathematical model with the experimental results reported in our previous publication [Geng and Park, 1994]. In the model, we included a growth parameter to count the cell activity loss due to cell aging or overcrowding effect [Contois, 1959] because we observed that cell growth in a fed-batch culture tended to slow down after an initial period [Geng and Park, 1994].

†Corresponding author

MATHEMATICAL MODEL FOR FED-BATCH BUTANOL FERMENTATION WITH PERVAPORATION

Fig. 1 shows a control volume of the system consisted of a fermentor and a pervaporation module mounted inside the fermentor. We developed mass balances for biomass concentration, substrate concentration, medium volume, and concentrations of five end products: butanol, acetone, ethanol, butyrate, and acetate.

1. Cell Growth and Mass Balance

In our fed-batch system, no cell mass was taken out of the fermentor and cell growth slowed down due to either accumulation of inhibitory products or aging effect of the overall cell population. To consider this effect, Monod's growth model was modified as follows by including a growth parameter, β [Contois, 1959] and a product inhibition term I:

$$\mu=\mu_{max}\frac{s}{\beta\chi+s}I \tag{1}$$

where μ is the specific cell growth rate, and μ_{max} is the maximum cell growth rate, s is glucose concentration, and χ is the biomass concentration, β is the growth parameter that, together with cell density (χ), serves as a Monod coefficient, and I is the butanol inhibition term. According to Costa and Moreira [1983], I was estimated as follows:

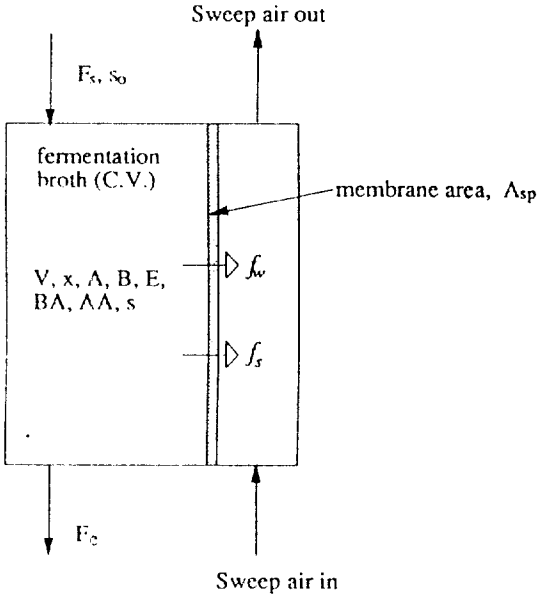

Fig. 1. Control volume applied to the fed-batch fermentation-separation system.
F_s: feed rate of supplemental medium, F_e: effluent rate, V: volume, x: cell mass concentration, A: acetone, B: butanol, E: ethanol, BA: butyric acid, AA: acetic acid, s: glucose concentration, f_w: volumetric water flux across the membrane, f_s: volumetric solvent loss due to pervaporation

$$I = 1 \qquad \text{when } C_B \le 4.5 \text{ g/L} \tag{2a}$$

$$I = 1.33 - 0.083\, C_B \qquad \text{when } C_B > 4.5 \text{ g/L} \tag{2b}$$

where C_B is butanol concentration in g/L. Notice that the butanol inhibition will not be in effect until butanol concentration goes beyond 4.5 g/L. For fed-batch pervaporative fermentation in which butanol concentration was about 4-5 g/L, the slow cell growth can only be explained by a growth parameter (β) that accounts for cell aging. Acid inhibition was not included in cell growth model because the strain we used (*Clostridium acetobutylicum* B18) was a low acid producer [Park et al., 1993]. The total cell mass, X, in the control volume, V(t), is given by:

$$X = V(t)\chi \tag{3}$$

where t is time and χ is cell mass concentration. The overall biomass balance is as follows:

$$\frac{dX}{dt} = \mu X - mX - F_e\chi \tag{4}$$

where μ is cell growth rate in Eq. (1) and m is maintenance rate. F_e is the effluent rate, which is zero if there is no bleeding during fermentation. Combining Eqs. (3) and (4) produces the following expression:

$$V\frac{d\chi}{dt} = (\mu - m)V\chi - F_e\chi - \frac{dV}{dt}\chi \tag{5}$$

The last term describes cell density decrease due to volume increase. The volume change with time is given below:

$$\frac{dV}{dt} = F_s - (f_w + f_s)A_{sp} - F_s \tag{6}$$

where F_s is the feed rate of medium supplement, A_{sp} is the surface area of the pervaporation module, f_w is the volumetric water flux across the membrane and is considered constant, f_s is the volumetric solvent loss due to pervaporation and is estimated by the following expression:

$$f_s = \frac{q_{sp}(B)}{\rho_b} + \frac{q_{sp}(A)}{\rho_a} + \frac{q_{sp}(E)}{\rho_e} \tag{7}$$

where q_{sp}'s and ρ's are the mass fluxes and densities for B (butanol), A (acetone) and E (ethanol), respectively. Eq. (7) relates volumetric flux rates with mass flux rates. q_{sp}'s are estimated as follows assuming flat membrane and zero concentration on the permeate (lumen) side of the membrane:

$$q_{sp}(i) = D_i\frac{C_i}{l} \tag{8}$$

where D_i and C_i are the diffusivity of component i through the silicone membrane and concentration of component i, respectively, and l is the membrane thickness.

Combining Eqs. (5) and (6) gives the cell mass balance equation as follows:

$$\frac{d\chi}{dt} = (\mu - m)x - \frac{F_s}{V}x - \frac{(f_w + f_s)A_{sp}}{V}\chi \tag{9}$$

The first term on the right hand side of Eq. (9) represents the cell mass concentration change due to growth and maintenance. The second term represents the dilution effect due to additional feed to the fermentor. Depending on the feed condition, F_s can be assigned zero or a specific value for certain period of time. The third term describes the concentrating effect due to volume loss of water and solvents by pervaporation. The effluent term F_e in Eq. (6) plays no role in the cell mass balance Eq. (5). This is true for the equations to follow. Physically this means that the concentration of an individual component in the fermentor does not change by broth withdrawal.

2. Butyrate Formation

Butyrate formation is growth-associated and is an efficient energy production process by *C. acetobutylicum* [Gottschalk, 1986]. When butyric acid concentration reaches a level, cells switch their biochemical pathway to solvent production. The decline of butyrate concentration during solventogenesis can be seen as an imbalance between butyrate production and its uptake. The uptake depends on pH, butyric acid concentration, and glucose availability [Geng et al., 1995; Fond et al., 1985], and is proportional to biomass concentration. A butyrate balance is given as follows:

$$\frac{dC_{BA}}{dt} = k_{ba}\mu\chi - (Sig)\,k_{bab}\frac{C_{uba}}{k_{c1} + C_{uba}}\frac{s}{k_s + s}\chi - \frac{F_s - (f_w + f_s)A_{sp}}{V}C_{BA} \tag{10}$$

where C_{BA} stands for butyrate concentration. On the right hand side of the equation, the first term represents the growth-associated butyrate production, the second term is the butyrate up-

take as a function of undissociated acid and glucose concentration, and the last term refers to the concentrating effect due to volume change. k_{ba} in the first term is the rate constant for butyrate formation. *Sig* in the second term indicates a physiological signal that switches on acid uptake and the solvent production when butyrate reached a certain concentration C_s. Thus *Sig* is given as follows:

$$Sig = 0 \text{ when } C_{BA} < C_s \tag{11a}$$

$$Sig = 1 \text{ when } C_{BA} \geq C_s \tag{11b}$$

where C_s depends on pH as follows [Geng, 1995]:

$$C_s = (0.48 - 0.176\text{pH})(1 + 10^{(pH - pK_a)}) \tag{11c}$$

Sig in the following Eqs. (13), (14) and (16) used the same definition as in Eq. (11). This was based on the assumption that butanol and acetone production was negligible before butyric acid concentration reaches C_s in Eq. (11). We also assumed that acetate uptake was synchronized with butyrate uptake. We think that these assumptions were reasonable because in our previous experiments butanol production was less than 1 g/L before butyric acid concentration started to decrease and onset of acetate uptake was 2-3 hrs behind the onset of butyrate uptake.

In the second term, k_{bab} is rate constant for butyrate uptake and k_{c1} is Monod coefficient for acid uptake, and C_{uba} is undissociated butyrate concentration and can be determined from the following Henderson-Hasselbach equation using a pK_a value of 4.82:

$$C_{uba} = \frac{10^{(pH - pK_a)}}{1 + 10^{(pH - pK_a)}} C_{BA} \tag{12}$$

3. Butanol Formation

For strain *C. acetobutylicum* B18, butanol formation showed a strong dependence on cell growth, and slight butanol production was observed in stationary phase [Park et al., 1993; Geng and Park, 1993]. Therefore, both growth associated and non-growth associated terms were used in this model for butanol formation similar to Srivastav et al. [1990]. The following equation describes butanol mass balance in the control volume:

$$\frac{dC_B}{dt} = Sig\left[(k_{b1}\mu + k_{b2})\chi + 0.841 k_{bab}\frac{C_{uba}}{k_{c1}} + C_{uba}\frac{s}{k_s + s}\chi\right] - q_{sp}(C_B)A_{sp} - \frac{F_s - (f_w + f_s)A_{sp}}{V}C_B \tag{13}$$

where C_B is butanol concentration, *Sig* is defined in Eq. (11). The first term on the right side of Eq. (13) is butanol formation rate in which k_{b1} and k_{b2} are rate constants for growth associated and non-growth associated butanol formation, respectively. The second term represents the butanol converted from butyrate. The constant 0.841 (g butanol/g butyrate) is the weight ratio of butanol and butyrate based on mole-to-mole conversion. The third term, $q_{sp}(C_B)$, represents butanol flux through the pervaporation module as indicated in Eq. (8). The last term describes the volume change effect.

4. Acetate Formation

Acetic acid formation is analogous to butyrate formation and acetate mass balance is given similar to butyrate mass balance:

$$\frac{dC_{AA}}{dt} = k_{aa}\mu\chi - (Sig)k_{aaa}\frac{C_{uaa}}{k_{c2} + C_{uaa}}\frac{s}{k_s + s}\chi - \frac{F_s - (f_w + f_s)A_{sp}}{V}C_{AA} \tag{14}$$

where k_{aa} is rate constant for acetate formation and k_{aaa} is rate constant for acetate uptake, and k_{c2} is Monod coefficient for acetate uptake. *Sig* is defined in Eq. (11). C_{uaa} is the undissociated acetate concentration at a given pH and pK_a of 4.76, and is given by the following expression:

$$C_{uaa} = \frac{10^{(pH - pK_a)}}{1 + 10^{(pH - pK_a)}}(C_{AA} - 0.5) \tag{15}$$

where a constant, 0.5 g/L, is subtracted from the total acetate concentration because experimental data showed that *C. acetobutylicum* B18 uptake acetate when its concentration was higher than 0.5 g/L [Park et al., 1993; Geng and Park, 1994].

5. Acetone Formation

Acetone mass balance is similar to butanol mass balance, and is given as below:

$$\frac{dC_A}{dt} = Sig\left[(k_{a1}\mu + k_{a2})\chi + 0.482\, k_{aaa}\frac{C_{uaa}}{k_{c2} + C_{uaa}}\frac{s}{k_s + s}\chi\right] - q_{sp}(C_A)A_{sp} - \frac{F_s - (f_w + f_s)A_{sp}}{V}C_A \tag{16}$$

The first term in the parenthesis on the right hand side is acetone formation, where k_{a1} and k_{a2} are rate constants for growth associated and non-growth associated acetone formation, respectively. The second term represents acetone converted from acetate. *Sig* is defined in Eq. (11). The constant, 0.482, is based on the assumption that two moles of acetate is needed to form one mole of acetone [Srivastava and Volesky, 1990]. The third term, $q_{sp}(C_A)$, refers to the acetone flux by pervaporation as shown in Eq. (8). The last term represents the volume change effect on the acetone concentration.

6. Ethanol Formation

Ethanol is produced during early stage of cell growth as a way of NADH oxidation (personal communication with Dr. David Woods, South Africa). Thus, ethanol formation is growth associated. Because ethanol production by the strain B18 is low [Park et al., 1993], the non-growth associated term is not included in this formulation. The ethanol mass balance is given as follows:

$$\frac{dC_E}{dt} = k_e\mu\chi - q_{sp}(C_E)A_{sp} - \frac{F_s - (f_w + f_s)A_{sp}}{V}C_E \tag{17}$$

where C_E is ethanol concentration, k_e is rate constant for growth-associated ethanol formation, $q_{sp}(C_E)$ is the ethanol separation flux as in Eq. (8), and the last term is the concentration variation due to volume change.

7. Substrate (glucose) Consumption

The substrate carbon balance is given below according to Roels [1983]:

$$\frac{ds}{dt} = \frac{1}{Y_{xs}}(\mu - m)x - \sum_1^5\left(\frac{1}{Y_i}\frac{dP_i}{dt}\right) - \frac{F_s(s_0 - s) + (f_w + f_s)A_{sp}s}{V} \tag{18}$$

where s is substrate (glucose) concentration; Y_{x} and Y_{i} are the cell mass yield and product i yield on glucose, respectively; dP_i/dt is the product formation rate for component i as described in Eqs. (10), (13), (14), (16), and (17), respectively; s_0 is the substrate concentration of the supplemental medium. The first term on the right hand side of Eq. (18) is the glucose consumption rate for biomass synthesis. The second term is the glucose conversion rate to acids and solvents. The last term refers to the glucose concentration change due to the volume change.

In summary, the model developed in this study consists of eight independent equations with eight unknowns. The unknowns are biomass concentration, substrate concentration, medium volume, and concentrations of five end products: butanol, acetone, ethanol, butyrate, and acetate. This system of first order differential equations is nonlinear and can be solved using Runge-Kutta method [Charpra and Canale, 1988]. A computer program for the Runge-Kutta method was written in PASCAL.

The model involves many constants that are not readily available. Their selection and sources are given in Table 1. Finding these coefficients requires the use of sophisticated software and the use of nonlinear regression technique [Volesky and Votruba, 1992].

Due to the limited information on our pervaporative fed-batch butanol system, some of the coefficients such as Monod coefficients were adopted from previous reports [Srivastava et al., 1990; Jarzebski et al., 1992] because they are less likely to affect the simulation results for a particular strain. Rate constants for acid and solvent formation were estimated from our batch and fed-batch fermentation results using a sequential parameter estimation method [Bailey and Ollis, 1986]. It should be pointed out that the yield factors in Eq. (18) are true yield factors [Roels, 1983] based on the biochemical pathways of the ABE fermentation and should not be confused with generic terms used in fermentation production analysis, which is defined as the products formed divided by the total glucose consumption during fermentation.

Table 1. List of coefficients used in the modeling

Item	Value	Explanation	References
β	25	Constant counting cell activity & density	Estimated
μ_{max}	0.26	Maximum cell growth rate	Jarzebski et al. [1992]
m	0.01	Maintenance rate	Jarzebski et al. [1992]
k_{ba}	1.11	Rate constant for butyrate formation	Estimated
k_{bab}	2.0	Rate constant for butyrate uptake	Estimated
k_{s1}	5.18	Monod coefficient for butyrate uptake	Volesky & Votruba [1992]
k_s	0.2	Monod coefficient for glucose concentration	Volesky & Votruba [1992]
k_{b1}	1.5	Rate constant for growth associated butanol formation	Estimated
k_{b2}	0.525	Rate constant for non-growth associated butanol formation	Estimated
k_{aa}	0.82	Rate constant for acetate formation	Estimated
k_{aaa}	0.5	Rate constant for acetate uptake	Estimated
k_{s2}	2.1	Monod coefficient for acetate uptake	Volesky & Votruba [1992]
k_{a1}	0.49	Rate constant for growth associated acetone formation	Estimated
k_{a2}	0.17	Rate constant for non-growth associated acetone formation	Estimated
k_e	0.1	Rate constant for ethanol formation	Estimated

RESULTS AND DISCUSSION

The prediction by the mathematical model was compared with our experimental data from batch fermentation with and without pervaporation, and fed-batch fermentation with pervaporation [Geng and Park, 1994]. Computer simulations were also carried out to show the effect of membrane area, membrane thickness, and sweep air flow rate on glucose consumption rate (GCR) and butanol concentration in the fermentation broth.

1. Model Prediction vs. Experimental Data in Batch Fermentation

Fig. 2 compares the results of model prediction and experimental data for batch fermentation without pervaporation (assign membrane area by zero, A_{sp}=0). Glucose concentration decreased slowly from an initial value of 60 g/L during the lag phase of biomass growth. With an increase in biomass and the onset of solventogenesis, glucose concentration decreased rapidly. This trend continued until the glucose was depleted and

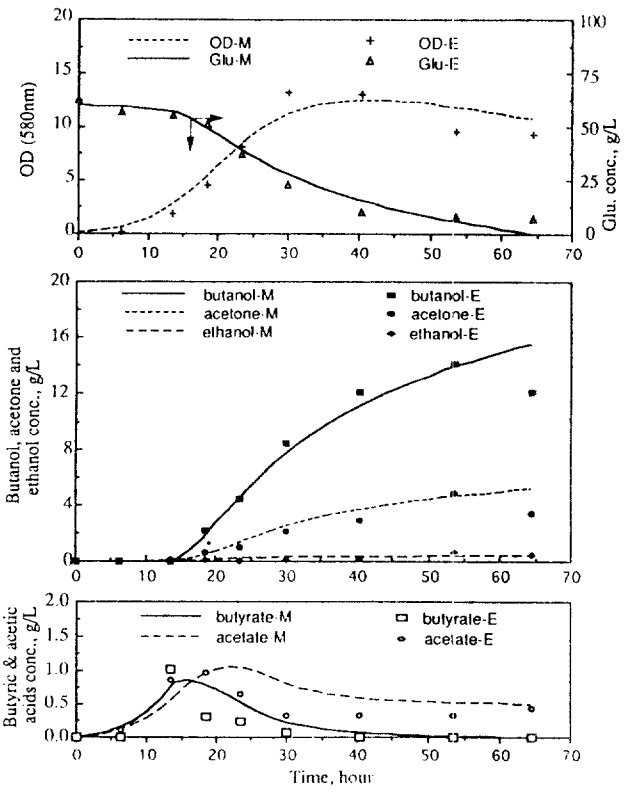

Fig. 2. Comparisons of model simulation (M) and experimental results (E) of a batch ABE fermentation without pervaporation using *C. acetobutylicum* B18.

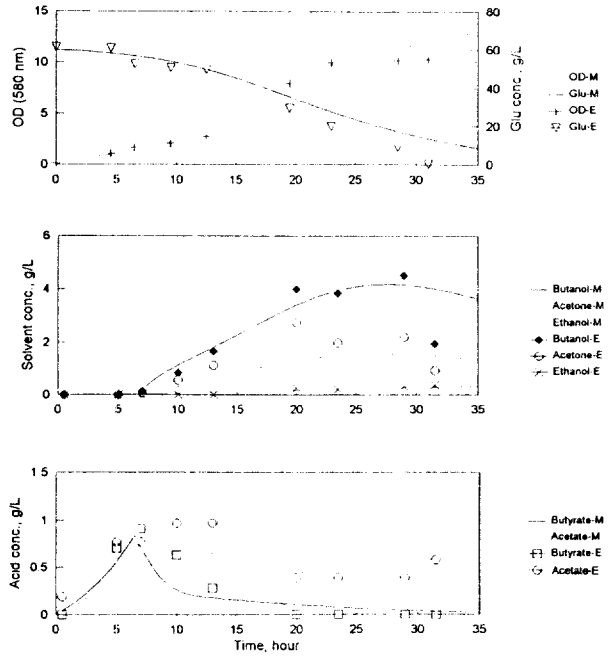

Fig. 3. Model simulation (M) compared with experimental data (E) in a batch ABE fermentation with pervaporation.

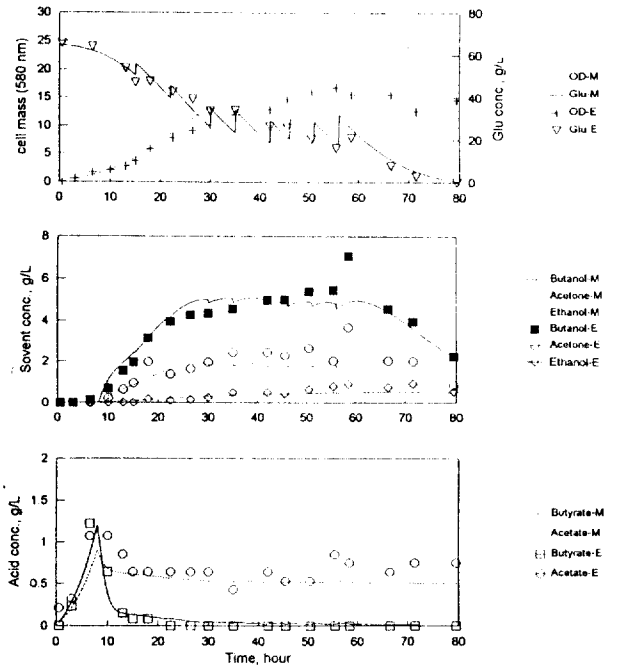

Fig. 4. Model simulation (M) compared with experimental data (E) of a fed-batch ABE fermentation with pervaporation.

cell growth was inhibited by the high butanol content in the medium. At hour 40, cell mass began to decrease due to cell autolysis. After that, butanol and acetone concentrations continued to increase until the glucose was completely consumed. During the whole fermentation period dependence of solvent production on cell growth was a mixed type, first growth-associated production followed by non-growth associated production when cell mass began to decrease at hour 40. The model predicted the final butanol concentration of 15.7 g/L. The butanol yield was 26%, which was similar to our experimental results [Park et al., 1993]. The predicted profiles matched well with the experimental data.

The results in Fig. 2 indicate that the model satisfactorily predicted formation and uptake of acids by *C. acetobutylicum* B18. The simulation showed that cells produced butyrate and acetate in the acidogenic phase and began to take up acids during the solventogenic phase. The model predicted the maximum butyrate concentration similar to the experimental results. Acetic acid uptake was slow, and its re-utilization was not favorable at concentrations less than 0.5 g/L. Notice the difference between the experimental and the predicted decline of acid concentrations, especially of acetate. This was probably caused by either over-estimating acid production or under-estimating acid uptake during solventogenesis.

2. Model Prediction vs. Experimental Data in Batch Fermentation with Pervaporation

Batch fermentation with pervaporation was simulated by assigning membrane area by 0.17 m^2 (A_{sp}=0.17) at the onset of butanol production. Fig. 3 shows the model simulation and experimental results for batch fermentation with pervaporation. In general, the model predicted the experimental data satisfactorily. The model was also able to predict the onset time of solvent production. The model predicted a complete butyrate uptake near the end of the simulation. Acetate concentration remained at 0.5 g/L during the rest of the fermentation because acetate uptake was designed to be effective only when its concentration exceeded 0.5 g/L.

3. Model Prediction vs. Experimental Data in Fed-batch Fermentation with pervaporation

Fig. 4 compares the experimental data with the model simulation during fed-batch fermentation with pervaporation (assign membrane area by 0.17 m^2, A_{sp}=0.17). The experimental data show the glucose concentration before each medium supplement. The amount of glucose supplemented to the medium was shown by the vertical increases in the simulated glucose concentration. Glucose concentration predicted by the model agreed well with the experimental data except some underestimation during hours 30 and 40. Cell mass predicted by the model appears overestimated because cell mass entrapped in the pervaporation module was not included in the experimental data. The product concentrations predicted by the model agreed well with the experimental data except for the sudden increase at hour 60, which was caused by an unexpected stoppage of pervaporation. Butyrate concentration predicted by the model matched satisfactorily with the experimental data. Acetate concentration was slightly underestimated at the onset point of solvent production, but its concentration showed a good agreement with the experimental data and was maintained at a level of 0.5 g/L. These results indicated that material balances used in the model equations were proper and the mechanisms involved in ABE fermentation by strain B18 were properly incorporated in the model.

4. The Effect of Membrane Area, Membrane Thickness, and Sweep Air Flow Rate on Glucose Consumption Rate and Residual Butanol Concentration in the Fermentation Medium

The efficiency of solvent removal from the medium in a fer-

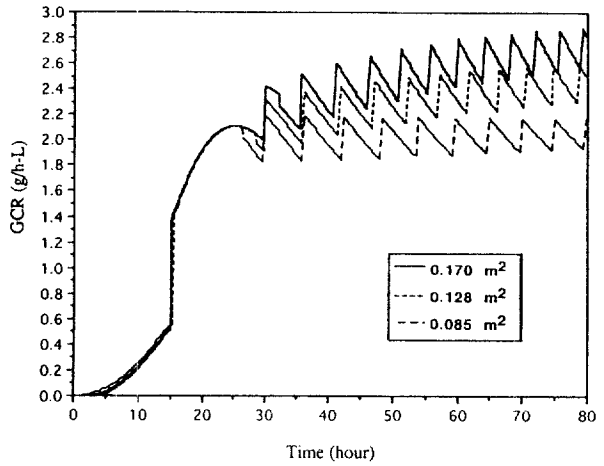

Fig. 5. Effect of membrane area on glucose consumption rate (GCR) during fed-batch fermentation and pervaporation.

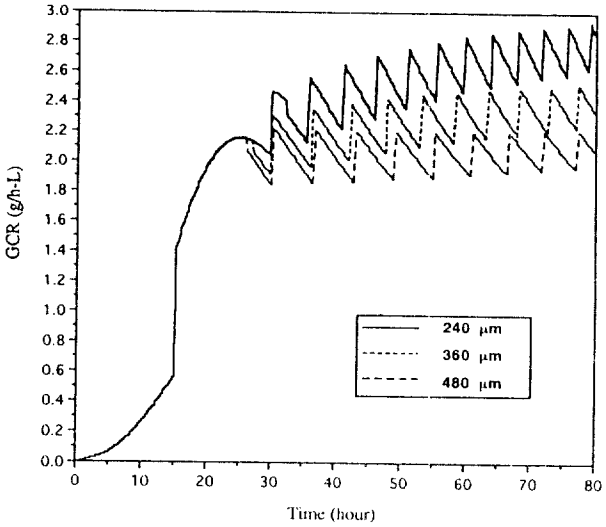

Fig. 6. Effect of membrane thickness on glucose consumption rate (GCR) during fed-batch fermentation and pervaporation.

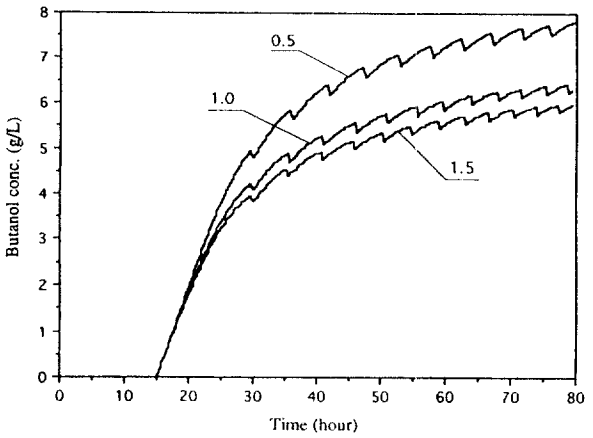

Fig. 7. Effect of sweep air flow rate on residual butanol concentraton during pervaporative fed-batch fermentation (unit for air flow rate: L/min/tubing).

mentation-pervaporation system depends on such factors as membrane area, membrane thickness, and sweep air flow rate. Efficient butanol removal will increase glucose consumption rate (GCR) defined as glucose consumed per liter broth per hour. The standard conditions used to study the effect of membrane area, membrane thickness and sweep air flow rate were as follows: membrane surface area 0.17 m^2, air flow rate 1 L/min-tubing, and membrane thickness 240 μm. For example, during surface area test, surface area was varied while membrane thickness and sweep air flow rate were fixed at 240 μm and 1 L/min-tubing, respectively.

Fig. 5 shows the dependence of GCR on membrane surface area. Three surface areas of 0.085, 0.128, and 0.17 m^2 were tested while keeping membrane thickness and sweep air flow rate constant. The slow rise in GCR during initial 15 hrs corresponds to before solvent production. The vertical increase at about 15th hour was caused by the onset of solvent formation. During typical batch butanol fermentation glucose consumption increases rapidly at the onset of solvent formation because butanol and acetone, the two major products, start to be produced at around this time. In our numerical calculation a vertical increase in glucose consumption rate (GCR) was also related to the use of *Sig* in Eqs. (10), (13), (14) and (16) which simultaneously turns on glucose consumption for butanol and acetone production when butyrate concentration reaches a critical level (C_c). In numerical calculation glucose consumption rate was calculated by dividing glucose consumption (g/L) by a small time interval (Δt) that was used for numerical integration. This resulted in an almost vertical increase in glucose consumption rate. After solvent formation started, GCR increased further. GCR decreased slightly when glucose concentration decreased below 30 g/L near the 25th hr. When glucose concentration was increased vertically by glucose supplements, GCR jumped to higher levels. As this process repeats, a saw-blade type of GCR profile resulted.

When the membrane area was doubled from 0.085 m^2 to 0.17 m^2, GCR increased by 30% (from 2.15 to 2.8 g/L-h at hour 80). Total glucose consumption also increased by 30% (from 100 g/L for 0.085 m^2 to 130 g/L for 0.17 m^2 during hours 29 and 80). As shown in Fig. 6, a thinner membrane increased glucose consumption. When membrane thickness was decreased by half (from 480 μm to 240 μm), the GCR increased by 33% (from 2.1 to 2.8 g/L-h). Total glucose consumption during hours 29 to 80 also increased by 33%, from 135 to 180 g/L.

Fig. 7 shows that residual butanol concentration decreases at higher sweep air flow rates. For example, at hour 80 the butanol concentration decreased from 8 g/L to 6 g/L when the sweep air flow rate increased from 0.5 L/min/tubing to 1.0 L/min/tubing. A further increase in air flow rate to 1.5 L/min/tubing decreased the butanol concentration only by 0.5 g/L. This is because the diffusion rate through the membrane does not increase significantly once the flow rate reached a certain critical point [Geng and Park, 1994]. Residual butanol concentration was similar from hour 15 to about 22. This means that even at a lower flow rate of 0.5 L/min/tubing butanol removal was effective as long as butanol concentration was less than 2 g/L.

CONCLUSIONS

The prediction by the mathematical model developed in this

study agreed well with the experimental data for batch fermentation with and without pervaporation and fed-batch fermentation with pervaporation. The model satisfactorily described the physiological principles involved in ABE fermentation and well represented the mass balances involved in the fermentation-separation process. The model predicted that doubling surface area increased glucose consumption rate (GCR) by 30% and decreasing thickness by half increased GCR by 33%. Increasing sweep air flow rate also increased separation efficiency, but to a limited extent.

ACKNOWLEDGMENTS

This work was supported by BIOTECH 2000 program (1995) of Korean Ministry of Science and Technology.

NOMENCLATURE

A : acetone [-]
AA : acetic acid [-]
A_{sp} : membrane area [m^2]
B : butanol [-]
BA : butyric acid [-]
C_A : acetone concentration [g/L]
C_{AA} : acetic acid concentration [g/L]
C_B : butanol concentration [g/L]
C_{BA} : butyric acid concentration [g/L]
C_E : ethanol concentration [g/L]
C_i : concentration of component i [g/L]
C_c : critical butyric acid concentration required for solvent production [g/L]
D_i : solvent diffusivity [m^2/hr]
E : ethanol [-]
f_s : volumetric solvent loss due to pervaporation [L/m^2-hr]
f_w : volumetric water flux across the membrane [L/m^2-hr]
F_e : effluent rate [L/hr]
F_s : feed rate of supplement medium [L/hr]
I : butanol inhibition term [-]
l : membrane thickness [m]
k_{ba} : rate constant for butyrate formation [-]
k_{bab} : rate constant for butyrate uptake [hr^{-1}]
k_{b1} : Monod coefficient for butyrate uptake [g/L]
k_s : Monod coefficient for glucose conc. [g/L]
k_{b1} : rate constant for growth-associated butanol formation [-]
k_{b2} : rate constant for non-growth associated butanol formation [hr^{-1}]
k_{aa} : rate constant for acetate formation [-]
k_{aaa} : rate constant for acetate uptake [hr^{-1}]
k_{a2} : Monod coefficient for acetate uptake [g/L]
k_{a1} : rate constant for growth associated acetone formation [-]
k_{a2} : rate constant for non-growth associated acetone formation [hr^{-1}]
k_e : rate constant for ethanol formation [-]
m : maintenance rate [hr^{-1}]
P_i : product i concentration [g/L]
q_{sp} : mass flux [g/m^2-hr]
s, s_0 : glucose concentration [g/L]
t : time [hr]
V : volume [L]
χ, X : cell mass concentration [g/L], cell mass [g]
Y_{sx} : cell mass yield on glucose [g/g]
Y_i : product i yield on glucose [g/g]

Greek Letters

β : growth parameter [-]
μ, μ_m : specific cell growth rate, maximum cell growth rate [hr^{-1}]
ρ : density [g/L]

REFERENCES

Bailey, H. and Ollis, D. F., "Biochemical Engineering Fundamentals", McGraw-Hill, New York, 1986.

Charpra, S. C. and Canale, R. P., "Numerical Methods for Engineers", McGraw Hill, New York, 1988.

Contois, D. E., "Kinetics of Bacterial Growth. Relationship between Population Density and Specific Growth Rate of Continuous Cultures", *J. of Gen. Microbiol.*, **21**, 40 (1959).

Costa, J. M. and Moreira, A. R., "Growth Inhibition for Kinetics of the Acetone-Butanol Fermentation", *Amer. Chem. Soc. Symp. Ser.*, **207**, 501 (1983).

Fond, O., Matta-El-Amouri, G., Petitdemange, H. and Engasser, J. M., "The Role of Acids on the Production of Acetone and Butanol by *Clostridium acetobutylicum*", *Appl. Microbiol. and Biotech.*, **22**, 195 (1985).

Geng, C., Ph.D. Dissertation, "Acetone-Butanol-Ethanol Fermentation and Pervaporation by *Clostridium acetobutylicum* B 18", University of Minnesota, St. Paul, U.S.A. 1995.

Geng, Q. and Park, C.-H., "Pervaporative Butanol Fermentation by *Clostridium acetobutylicum* B18", *Biotech. Bioeng.*, **43**, 978 (1994).

Geng, Q. and Park, C.-H., "Controlled-pH Batch Butanol-Acetone Fermentation by a Low Acid Producing *Clostridium acetobutylicum* B18", *Biotech. Lett.*, **15**, 421 (1993).

Geng, Q., Park, C.-H. and Janni, K. A., "Uptake of Organic Acids by *Clostridium acetobutylicum* B18 under Controlled pH and Reduced Butanol Inhibition", *Korean J. of Chem. Eng.*, **12**, 378 (1995).

Gottschalk, G., "Bacterial Metabolism", Springer-Verlag, NY, 1986.

Groot, W. J., den Reyer, M. C. H., van der Lans, R. G. J. M. and Luyben, K. Ch. A. M., "Integration of Pervaporation and Continuous Butanol Fermentation with Immobilized Cells II: Mathematical Modeling and Simulations", *Chem. Eng. J.*, **46**, B11 (1991).

Jarzebski, A. B., Goma, G. and Soucaille, P., "Modelling of Continuous Acetonobutylic Fermentation", *Bioproc. Eng.*, **7**, 357 (1992).

Park, C.-H., Geng, Q. and Rogers, P., "Characteristics of Butanol Fermentation by a Low-Acid-Producing *Clostridium acetobutylicum* B18", *Appl. Microbiol. and Biotech.*, **39**, 148 (1993).

Park, C.-H., Okos, M. R. and Wankat, P. C., "Acetone-Butanol-Ethanol (ABE) Fermentation and Simultaneous Separation in a Trickle Bed Reactor", *Biotech. Prog.*, **7**, 185 (1991).

Roels, J. A., "Energetics and Kinetics in Biotechnology", Elsevier Biomedical Press, New York, 1983.

Shukla, R., Kang, W. and Sirkar, K. K., "Acetone-Butanol-Ethanol (ABE) Production in a Novel Hollow Fiber Fermentor-Extractor", *Biotech. Bioeng.*, **34**, 1158 (1989).

Srivastava, A. K. and Volesky, B., "Updated Model of the Batch Acetone-Butanol Fermentation", *Biotech. Lett.*, **12**, 693 (1990).

Volesky, B. and Votruba, J., "Modeling and Optimization of Fermentation Processes", Elsevier, New York, 1992.

Votruba, J., Volesky, B. and Yerushalmi, L., "Mathematical Model of a Batch Acetone-Butanol Fermentation", *Biotech. Bioeng.*, **28**, 247 (1986).